

**Supplementary Information for:**

**Butyrate extends health and lifespan in mice with  
mitochondrial deficiency**

Enrique Gabandé-Rodríguez<sup>†</sup>, Manuel M. Gómez de las Heras<sup>†</sup>, Pablo Ramírez-Ruiz de Erenchun, Carolina Simó, Virginia García-Cañas, Naohiro Inohara, Inés Berenguer-López, Violeta Enríquez-Zarralanga, Álvaro Fernández-Almeida, Jorge Oller, Gonzalo Soto-Heredero, Elisa Carrasco, Cristina Vázquez-Muñoz, Sandra Delgado-Pulido, José Ignacio Escrig-Larena, Isaac Francos-Quijorna, Raquel Justo-Méndez, Juan Francisco Aranda, Joanna Poulton, Ana Victoria Lechuga-Vieco, José Antonio Enríquez, Gabriel Núñez and María Mittelbrunn\*

<sup>†</sup> These authors contributed equally to this work

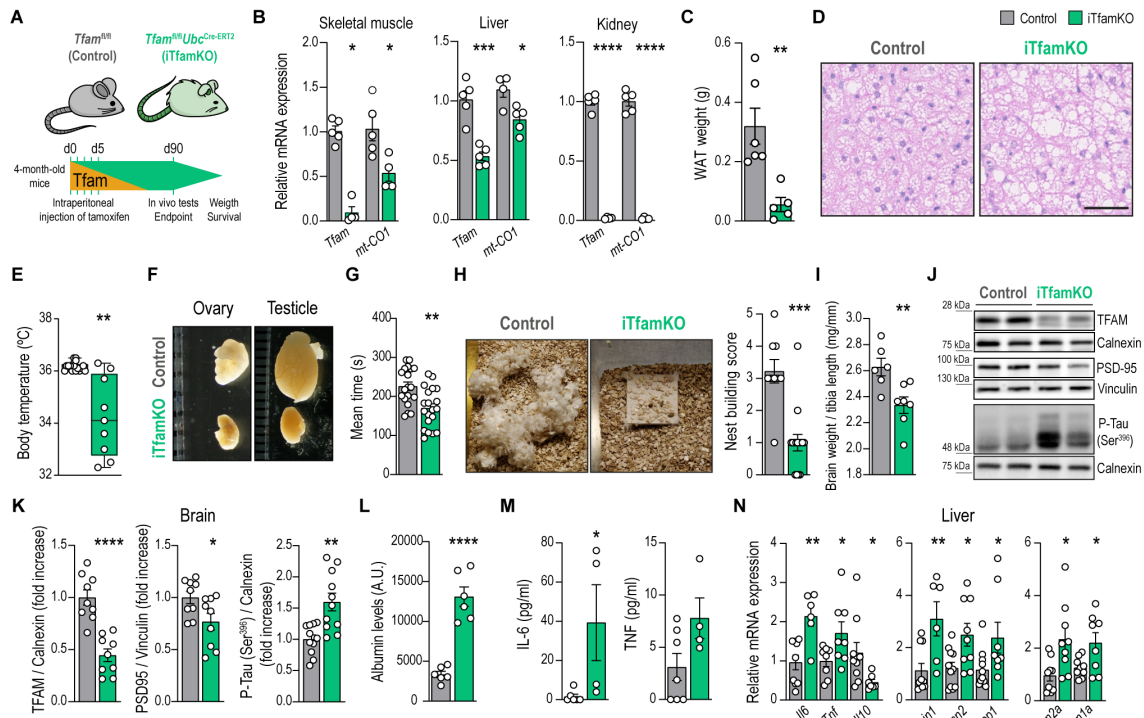
\* Corresponding author. Email: [mmittelbrunn@cbm.csic.es](mailto:mmittelbrunn@cbm.csic.es)

**This PDF file includes:**

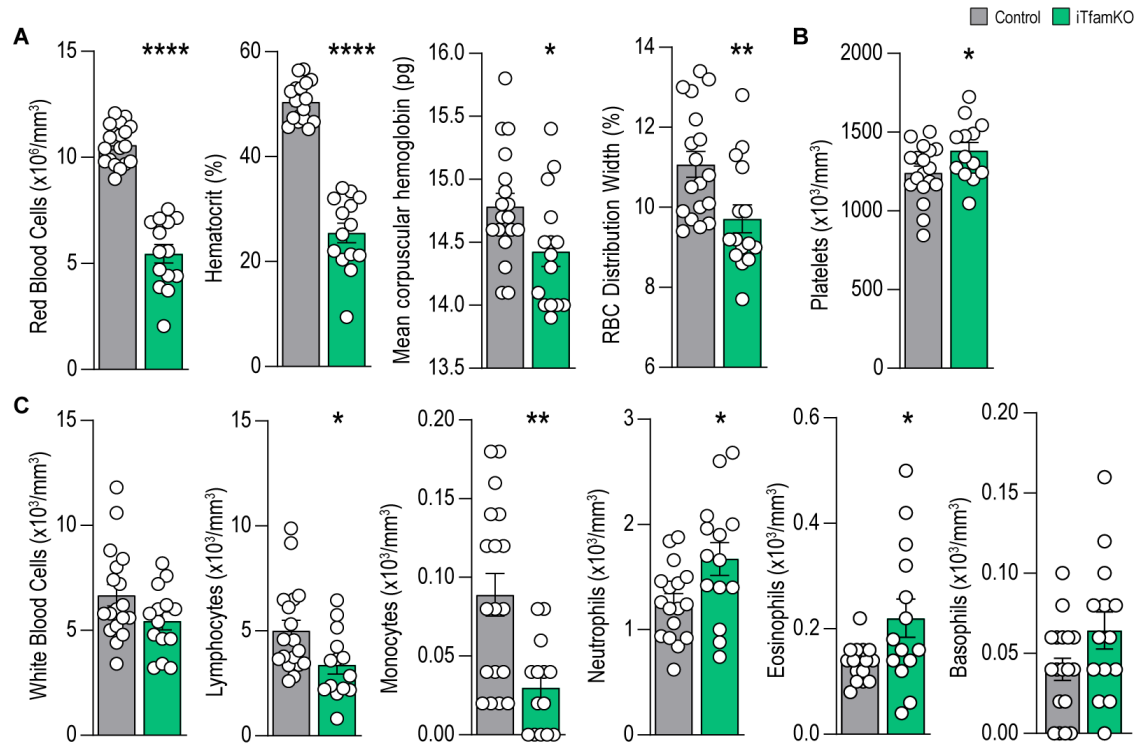
Figures S1 to S10.

Tables S1 and S2.

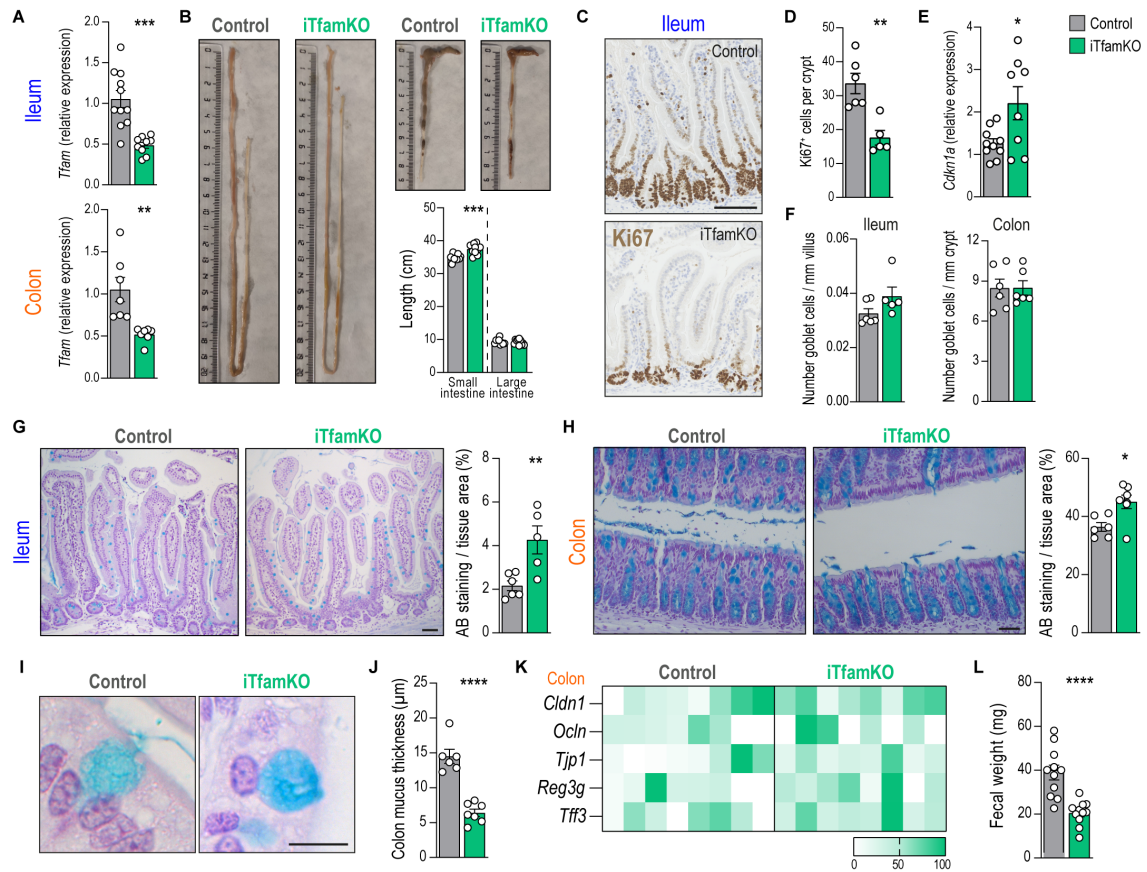
Uncropped scans of blots shown in Supplementary Figures.



**Figure S1. Inducible deletion of *Tfam* in adult mice precipitates multimorbidity.** (A) Experimental design of tamoxifen inducible deletion of *Tfam* in adult mice. (B) Relative mRNA levels of *Tfam* in the skeletal muscle, liver, and kidney of control and iTfamKO mice ( $n = 4$  to 5). (C) Quantification of gonadal white adipose tissue (WAT) weight ( $n = 5$  to 6). (D) Representative hematoxylin and eosin-stained sections of brown adipose tissue. Scale bar: 50  $\mu$ m. (E) Quantification of mouse body temperature ( $n = 9$  to 16). (F) Representative picture of mouse gonads. (G) Rotarod test performance expressed as the mean time spent on the rotating rod in all trials combined ( $n = 19$  to 20). (H) Representative picture of a mouse nest and its respective score ( $n = 3$  to 5). (I) Quantification of brain weight normalized to tibia length ( $n = 6$  to 7). (J) Representative immunoblot of TFAM, PSD-95, and phospho-Tau (Ser396) proteins in brain samples. (K) Densitometry analysis of brain immunoblots ( $n = 8$  to 12). (L) Quantification of albumin levels in urine ( $n = 6$ ). (M) Concentration of IL-6 and TNF in the serum ( $n = 4$  to 7). (N) Relative mRNA levels of genes encoding inflammatory mediators (*Il6*, *Tnf*, *Il10*), pro-fibrotic factors (*Serpin1*, *Ccn2*, *Spp1*), and senescence-associated markers (*Cdkn2a*, *Cdkn1a*) in the liver ( $n = 6$  to 11). All experiments were performed 90-days post-tamoxifen injection. Data are shown as means  $\pm$  SEM, where each dot is a biological sample.  $P$  values were determined by (B, C, G, I, and K to N) unpaired two-tailed Student's  $t$  test, (E) Wilcoxon test or (H) two-tailed Mann-Whitney  $U$  test. \* $P \leq 0.05$ ; \*\* $P \leq 0.01$ ; \*\*\* $P \leq 0.001$ ; and \*\*\*\* $P \leq 0.0001$ . Source data and exact  $P$  values are provided as a Source Data file.



**Figure S2. iTfamKO mice exhibit severe alterations in the hematopoietic cell compartment.** (A) Quantification of hematologic parameters related to red blood cell (RBC) biology in control and iTfamKO mice ( $n = 14$  to  $18$ ). (B) Quantification of blood platelets ( $n = 13$  to  $18$ ). (C) Quantification of hematologic parameters related to white blood cell biology ( $n = 14$  to  $18$ ). All experiments were performed 90-days post-tamoxifen injection. Data are shown as means  $\pm$  SEM, where each dot is a biological sample.  $P$  values were determined by (A to C) unpaired two-tailed Student's  $t$  test. \* $P \leq 0.05$ ; \*\* $P \leq 0.01$ ; and \*\*\*\* $P \leq 0.0001$ . Source data and exact  $P$  values are provided as a Source Data file.





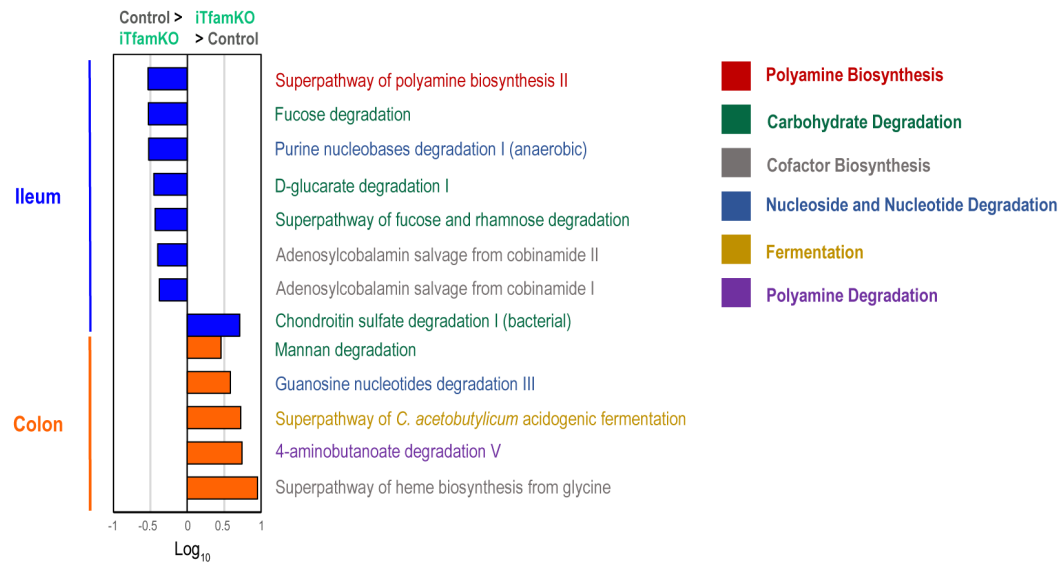


**Figure S4. Predictive metabolic profiling of the intestinal microbiota in iTfamKO mice.** PICRUSt2 prediction of metabolic pathways in ileal and colonic metagenomic data of control and iTfamKO mice (FDR,  $Q < 0.05$ ;  $|\text{SNR}| > 0.5$ ;  $|\text{LDA}| > -1$ ;  $|\text{fold change}| > 2$ ; maximal index  $> 1000$ ). Source data are provided as a Source Data file.

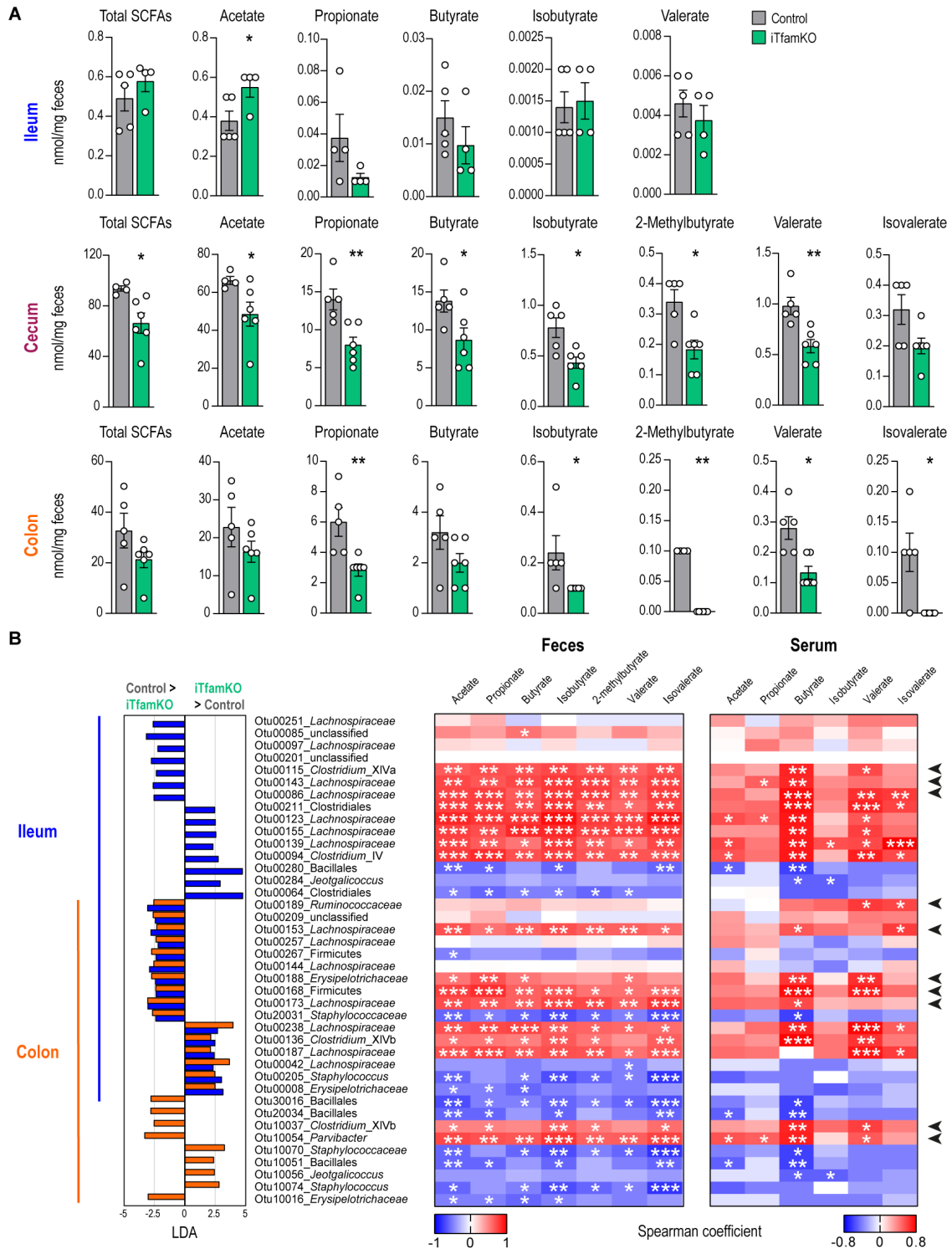


**Figure S5. Evaluation of short-chain fatty acids (SCFAs) in the intestine of iTfamKO mice.** (A) Quantification of SCFAs in the contents of the ileum, the cecum, and the colon of control and iTfamKO mice ( $n = 4$  to  $6$ ). (B) Left: differentially abundant operational taxonomic units (OTUs) depicted with lineal discriminant analysis (LDA) values of linear discriminant effect size (LEfSe,  $P < 0.05$ ; FDR,  $Q < 0.05$ ;  $|\text{SNR}| > 0.5$ ;  $|\text{LDA}| > 2$ ;  $|\text{fold change}| > 10$ ; maximal abundance  $> 0.001$ ) comparing the ileum and colonic microbiota in control versus iTfamKO mice. Right: heatmap depicting Spearman's rank correlation coefficients between differentially abundant OTUs in ileal and colon-resident microbiota,

and the concentration of SCFAs in the feces and the serum of mice. All experiments were performed 90-days post-tamoxifen injection. Data are shown as means  $\pm$  SEM, where each dot is a biological sample. *P* values were determined by (A) unpaired two-tailed Student's *t* test or two-tailed Mann-Whitney *U* test, or (B) PICRUST2 software. \**P*  $\leq$  0.05; \*\**P*  $\leq$  0.01; and \*\*\**P*  $\leq$  0.001. Source data are provided as a Source Data file.

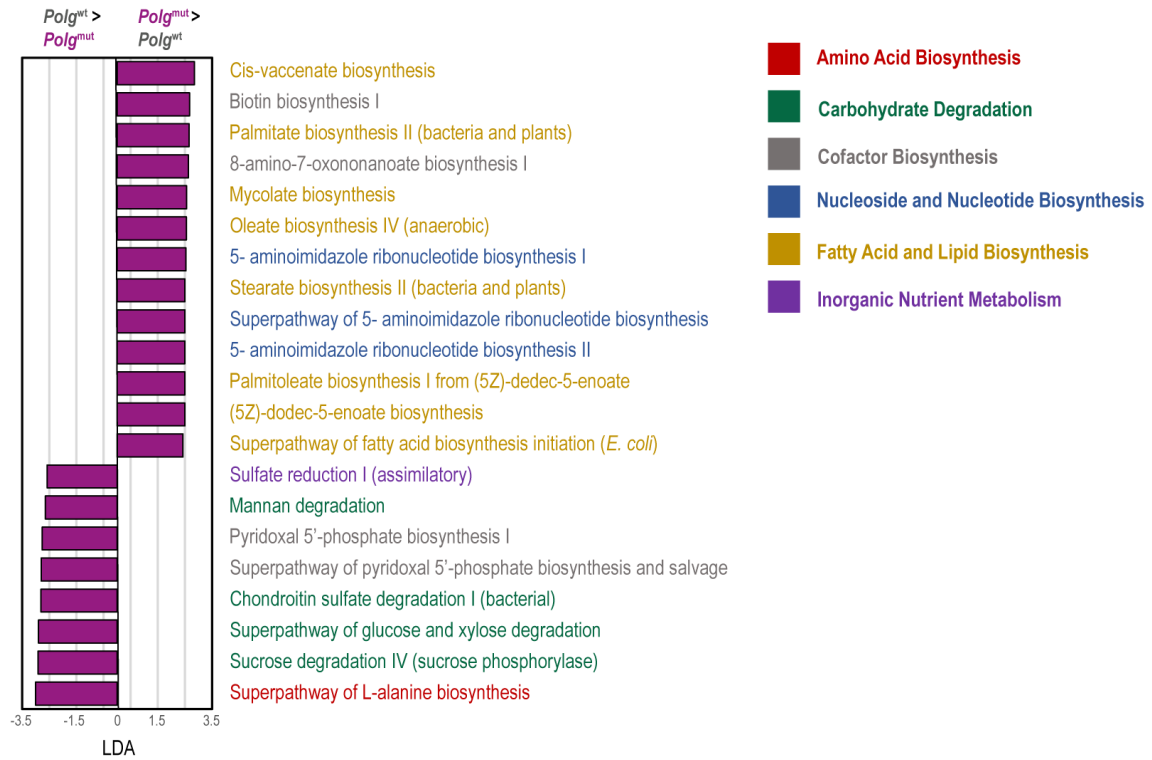


**Figure S6. Predictive metabolic profiling of fecal microbiota in mtDNA-mutator mice.** PICRUSt2 prediction of metabolic pathways in fecal metagenomic data of control and *Polg<sup>mut</sup>* mice (FDR,  $q < 0.05$ ; |SNR| > 1; |LDA| > 2). Source data are provided as a Source Data file.

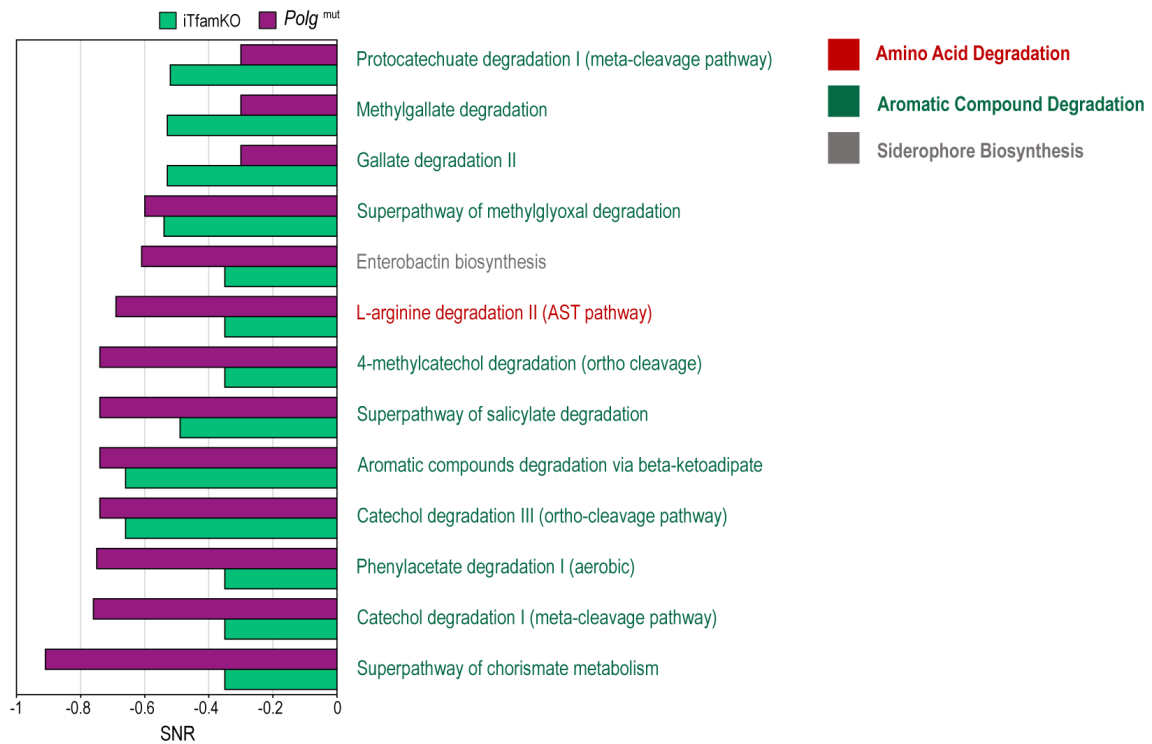


**Figure S7. Predictive metabolic profile of intestinal microbiota shared by iTfamKO and mtDNA-mutator mice.** PICRUST2 prediction of shared metabolic pathways in metagenomic data of iTfamKO and *Polg*<sup>mut</sup> mice (FDR,  $q < 0.05$ ; |SNR|  $> 0.2$ ; |LDA|  $> -1$ ; |fold change|  $> 1$ ; maximal abundance  $> 0$ ). Source data are provided as a Source Data file.

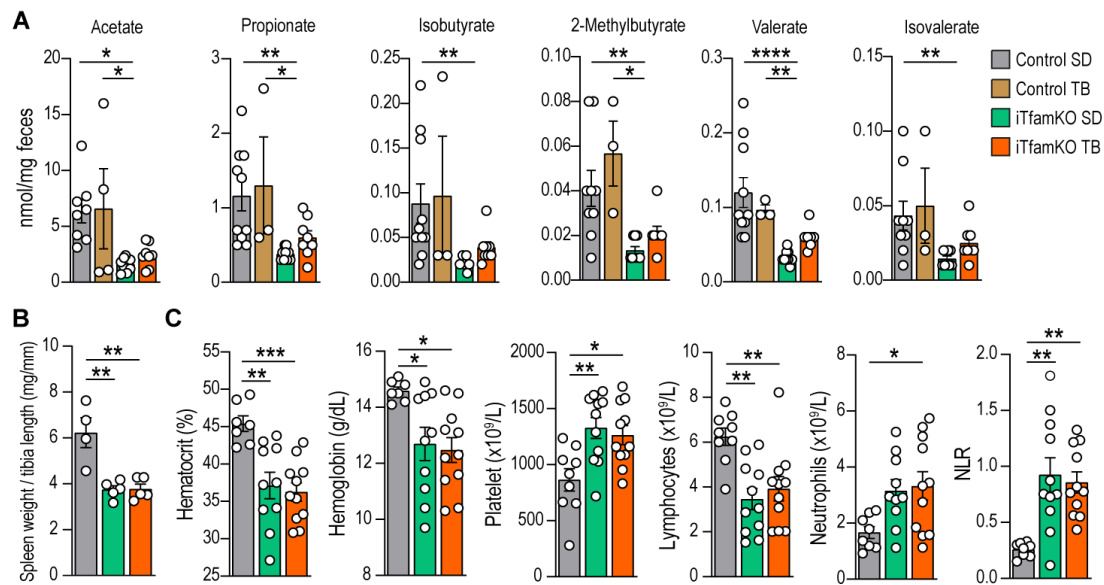


**Figure S8. Analysis of short-chain fatty acids (SCFAs) and hematological parameters in iTfamKO mice after tributyrin administration.** (A) Quantification of SCFAs in the feces of control and iTfamKO mice fed either a standard diet (SD) or a 10% tributyrin-supplemented diet (TB) ( $n = 3$  to 10). (B) Quantification of spleen weight normalized to tibia length ( $n = 4$  to 5). (C) Quantification of hematological parameters related to red blood cells, platelets, and white blood cells ( $n = 7$  to 11). Data are shown as means  $\pm$  SEM, where each dot is a biological sample.  $P$  values were determined by (A to C) one-way analysis of variance (ANOVA) with Tukey's multiple comparisons test. \* $P \leq 0.05$ ; \*\* $P \leq 0.01$ ; \*\*\* $P \leq 0.001$ ; and \*\*\*\* $P \leq 0.0001$ . Source data and exact  $P$  values are provided as a Source Data file.



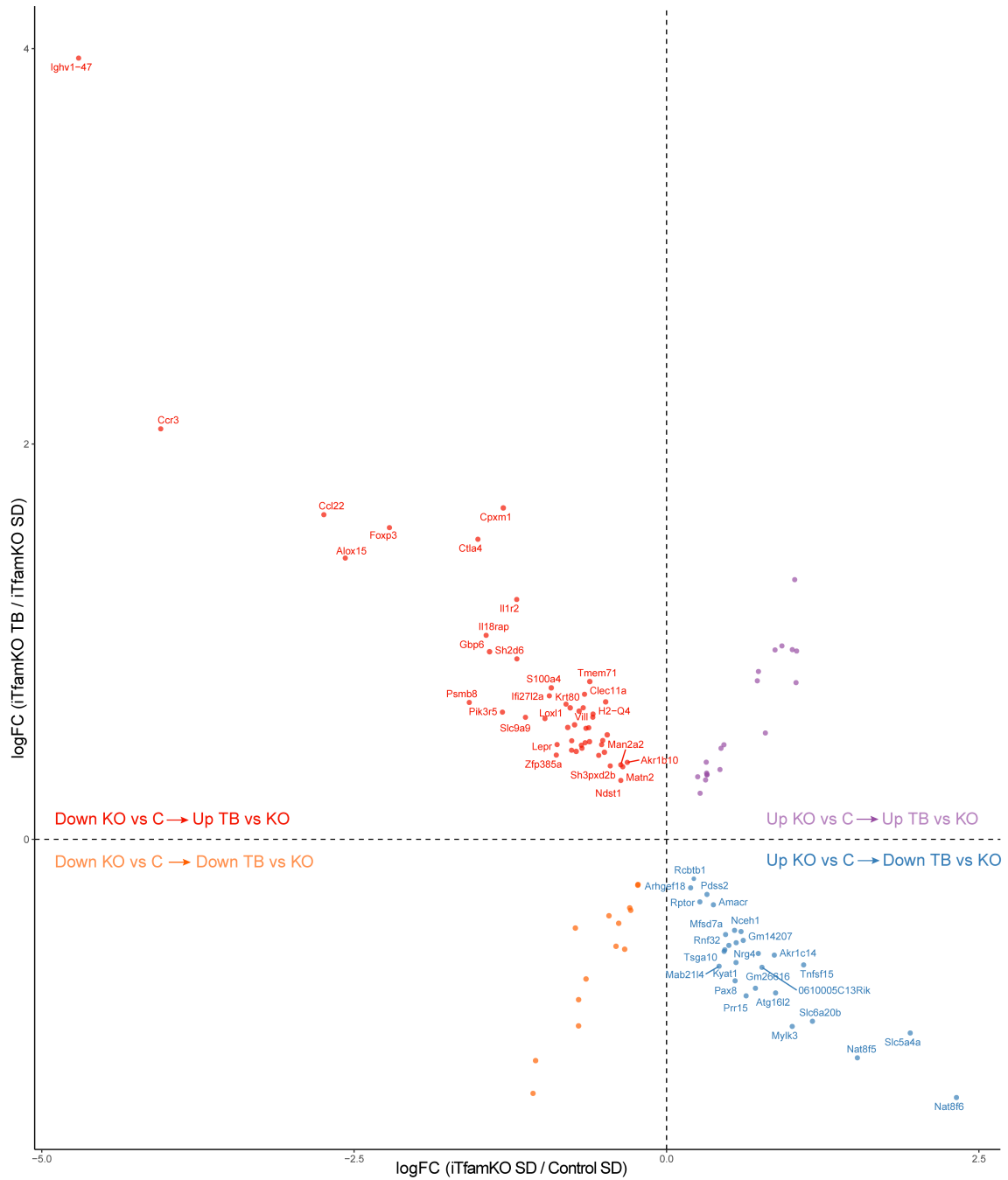


**Figure S9. Differentially expressed genes in the ileum of iTfamKO mice after tributyrin administration.** Four-quadrant scatter plot depicting differentially expressed genes in the ileum RNA-sequencing analysis of iTfamKO mice fed either a standard diet (SD) or a 10% tributyrin-supplemented diet (TB).

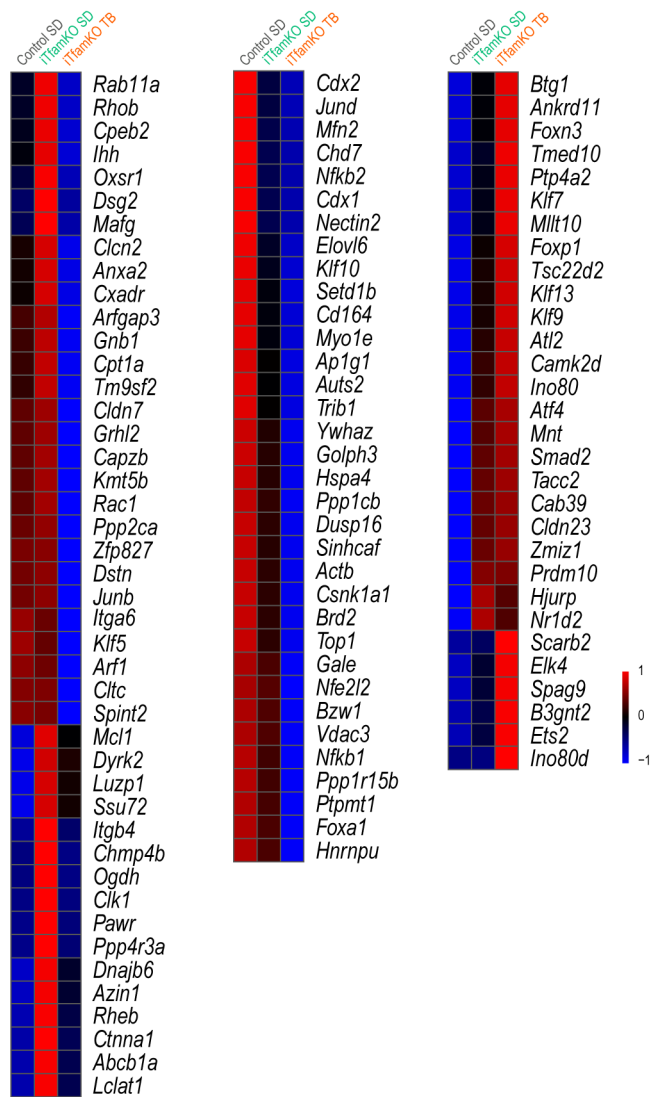


**Figure S10. Expression of H3K27bu-dependent genes in the RNA-sequencing analysis of the ileum of iTfamKO mice after tributyrin administration.** Heatmap depicting expression of H3K27bu-dependent genes in the ileum RNA-sequencing analysis of iTfamKO mice fed either a standard diet (SD) or a 10% tributyrin-supplemented diet (TB).

**Table S1. Primers for qPCR analysis of mouse intestines.**

Gene	Oligonucleotide (FW)	Oligonucleotide (RV)
<i>Tfam</i>	CAGGAGGCAAAGGATGATTC	CCAAGACTTCATTTTCATTGTCTG
<i>Mt-CO1</i>	CTCGCCTAATTTATTCCACTTCA	GGGGCTAGGGGTAGGGTTAT
<i>Gdf15</i>	CAACCAGAGCCGAGAGGAC	TGCACGCGGTAGGCTTC
<i>Mthfd2</i>	AGGTCCCAAGCCTTTGAGTT	GTAAGGGAGTGCCGTTGAAA
<i>Cdkn1a</i>	CTGACAGATTTCTATCACTCC	TTAAGACACACAGAGTGAGG
<i>Cdkn2a</i>	CCCGCCTTTTTCTTCTTAG	TTTCTCATGCCATTCCTTTC
<i>Tnf</i>	CTATGTCTCAGCCTCTTCTC	CATTTGGGAACCTCTCATCC
<i>Il6</i>	GTCTATAACCACTTCACAAGTC	TGCATCATCGTTGTTTCATAC
<i>Il10</i>	TGCCTTCAGCCAGGTGAAGACTTTC	CTTGATTTCTGGGCCATGCTTCTCTG
<i>Serpine1</i>	CCAACATCTTGGATGCTGAA	GCCAGGGTTGCACTAAACAT
<i>Ccn2</i>	AACTTCATGGATGGCCTCAAA	ACCCGGCTGCAGCTTGT
<i>Spp1</i>	ATGAGATTGGCAGTGATTTG	CATCCTTTTCTTCAGAGGAC
<i>Cldn1</i>	TCTACGAGGGACTGTGGATG	TCAGATTCAGCAAGGAGTCG
<i>Ocln</i>	GCTGTGATGTGTGTGAGCTG	GACGGTCTACCTGGAGGAAC
<i>Tpjl</i>	AGGACACCAAAGCATGTGAG	GGCATTCTGCTGGTTACA
<i>Defa5</i>	CTCCTCTCTGCCCTTGTCTT	GATTTCTGCAGGTCCCAAAA
<i>Defensin</i>	GGTGATCATCAGACCCCAGCATCAGT	AAGAGACTAAAACTGAGGAGCAGC
<i>Crypt1</i>	TCAAGGGCTGCAAAGGAAGAGAAC	TGGTCTCCATGTTTCAGCGACAGC
<i>Lyz1</i>	GAGACCGAAGCACCGACTATG	CGGTTTTGACATTGTGTTTCGC
<i>Ang4</i>	GGTTGTGATTCTCCTCAACTCTG	CTGAAGTTTTCTCCATAAGGGCT
<i>Reg3g</i>	ATGCTTCCCCGTATAACCATCA	GGCCATATCTGCATCATACCAG
<i>Tff3</i>	TTGCTGGGTCTCTGGGATAG	TACACTGCTCCGATGTGACAG
<i>Hprt</i>	TCCTCCTCAGACCGCTTTT	CCTGGTTCATCATCGCTAATC
<i>Pp1a</i>	ACGCCACTGTCGCTTTTC	GCAAACAGCTCGAAGGAGAC
<i>B2m</i>	TACATACGCCTGCAGAGTTAAGCA	TGATCACATGTCTCGATCCAG

**Table S2. Optimization of multiple reaction monitor (MRM) condition acquisition modes by direct infusion of 3-nitrophenylhydrazine (3NPH) derivatives.**

<b>3NPH-SCFA derivatives</b>	<b>Precursor ion (m/z)</b>	<b>Product ion (m/z)</b>	<b>Fragmentor voltage (V)</b>	<b>Collision energy (eV)</b>
AA (C2)	194.1	<b>137</b> 46	92	<b>16</b> 44
PA (C3)	208.1	<b>137</b> 46	92	<b>20</b> 48
i-BA/BA (C4)	222.1	<b>137</b> 107	92	<b>20</b> 28
2-Me-BA/i-VA/VA (C5)	236.1	<b>137</b> 107	102	<b>20</b> 32
2-Me-VA (C6)	250.1	<b>137</b> 107	102	<b>20</b> 31

**Uncropped scans of blots shown in Supplementary Figures.**

Relative to Fig. S1

